Fabrication and characterization of mesh electronics and in vitro metal electrode arrays

Jan Henk Davenschot, NanoElectronics, University of Twente, Enschede

***Abstract*—This paper presents the fabrication of mesh electronics and the design, fabrication and characterization of metal electrode arrays and elaborates on encountered fabrication issues and how they were or could be solved. The metal electrode arrays were designed with the aim of studying the relation between electrode radius and electrode impedance. To study the effect of material composition on recording cell cultivation is performed. A gold electrode sample with multiple electrode radii from 50μm to 2 μm was found to exhibit an exponential RMS noise dependence. However this was only measured one device and more data is needed to verify the accuracy of this trend.**

***Index Terms*—Mesh Electronics, Metal Electrode arrays, micro fabrication, Cell cultivation, Impedance measurements**

I. Introduction

The human brain is one of the most complex structures known to humanity. Estimates are that the brain consist of around 86 billion neurons forming around 100 trillion connections. Although much progress in understanding the brain been made over the past decades by the introduction of new non-invasive and invasive measurement techniques. Techniques such as MRI have proven their usefulness is studying active parts of the brain in vivo. This technique provides neuro scientist with a means to study the active regions of the brain. This technique however falls short to measure the deeper regions of the brain at a cellular level. It does not have sufficient resolution to measure the behaviour of neurons at a cellular level.

To measure the the behaviour of neurons at a a cellular of the brain scientist thus have to turn to invasive means such as metal electrodes to be able to measure and understand the deeper regions of the brain. Most brain electrodes have a major drawback to them because their implantation damages the tissue around the electrode due to a mismatch in bending stiffness between probe and tissue [1]. The insertion damage also leads to another negative side effect for electrophysiology studies as the tissue heals it creates scar tissue around the electrode which consequently limits also the recording stability of the electrode as the scar tissue separates the electrode from the neurons. [2]

The design and fabrication of such brain electrodes has been a continuously improving process. The advancements in nanotechnology over the past decades have enabled the fabrication of ever more complex and sophisticated brain electrodes such as Neuropixel, 3D silicon probes. Recently researchers at Lieberlab part of Harvard University have introduced mesh electronics as a new platform to study the brain. This platform has been designed with the specific aim of minimizing the insertion damage of the electrode. To achieve this the electrode has been designed to be of similar mechanical properties as the brain tissue. To that aim the the bending stiffness of the electrode was designed to be comparable with that of the brain tissue which limits micromotion between the electrode and tissue. Their results show the ability to track single neuron on the timescale of at least one year. [3]

The mesh electronics platform still makes use of conventional metal electrodes for recording neural signals. There have been suggestions to change the metal electrodes with actively switching components such as nanowire FETs to improve their sensitivity and spatial resolution further [1]. The work in this paper aims to investigate effect of size and material on electrodes. To this end multiple devices are fabricated and characterized.

The first devices that were fabricated were the state of the art of mesh electrodes. These devices were made with the aim of reproducing the results presented by the scientist of lieberlab aswell as to lay the ground work for possible further research which is envisioned to incorporate nanowire FET's instead of metal electrodes. To compare the measurement sensitivity of both recording devices it is required that both be fabricated and tested. For this animal studies are done in cooperation with the Raboud university of Nijmegen.

The second type of devices were metal electrode arrays (MEA's). These devices were designed and fabricated with multiple purposes. One was to to measure the effect of electrode size on electrode impedance. Impedance is the main cause for measurement noise which in turn is the main limiting factor for shrinking the size of recording electrodes. If the electrode size could be shrunk further this would allow for a higher density of electrodes and thus lead to an increased recording density.

It has been shown that a lower electrode impedance could be achieved modifying the surface properties of the

electrodes [4]. Typical electrodes materials used for invasive brain studies are made of gold or platinum [5]. As such it is aimed to compare the performance of gold and platinum for impedance measurements and cultivate cells on top of these devices such that in vitro recording resolution can be studied.

II. Theory

A. Electrochemical impedance spectroscopy

To measure the impedance of electrodes use is made of electrochemical impedance spectroscopy. The behavior of metal electrodes in an electrolyte solution is described by the circuit in figure 1. This model includes a double layer capacitance C_{dl} in parallel with a charge transfer resistance Rel to model an electrode. R_{sol} is the resistance of the solution. R_{ref}, C_{ref} are the resistance and capacitance of the external reference electrode respectively and have the same physical nature as the charge transfer resistance and the double layer capacitance.

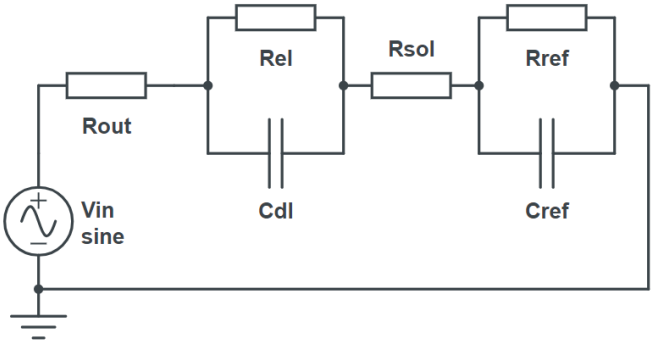

Fig. 1. Equivalent circuit modeling an electrode and external reference electrode submerged in a liquid solution. With an ideal voltage source output resistance R_{out}

$$R_{eq} = R_{EL}//\frac{1}{j\omega C_{dl}} + R_{sol} + R_{ref}//\frac{1}{j\omega Cref} \quad (1)$$

To measure the impedance the metal electrode array is submersed in a solution of PBS. Then the response to an external sine wave is measured. Using the transfer function and the measured response magnitude and phase response, the impedance of the electrodes can be measured. Furthermore, the resistance of the reference electrode should be minimized therefore it is typically made larger than the electrode that one aims to characterize.

B. Noise

As mentioned in the introduction the main limiting factor for shrinking the electrode size is the level of Johnson noise and is given by the following equation [6].

$$\overline{V_T^2} = 4k_bTR\Delta f \quad (2)$$

In which K_b is Boltzmann's constant, T temperature, R the resistance of the electrode and Δf the measurement bandwidth.

From this equation it is clear that in order to limit the amount of Johnson noise in an electrode the resistance of the electrode should be minimized. Considering that resistance scales inversely proportional with surface area (eq 3)

$$R = \frac{\rho L}{A} \quad (3)$$

The surface area scales quadratically with the radius of the electrodes. Thus obtaining equation

$$\overline{V_T^2} = 4k_bT\frac{\rho L}{\pi r^2}\Delta f \quad (4)$$

Thus obtaining for the RMS noise value:

$$\overline{V_T} = \frac{1}{r}\sqrt{4k_bT\frac{\rho L}{\pi}\Delta f} \quad (5)$$

One thus obtains that the amount of RMS Johnson noise should scale inversely proportional as a function of electrode radius.

III. Design

A. Mesh electronics

The supporting structure of the mesh is made out of SU-8 2000.5 photoresist. This photoresist is well suited for this application because of its favourable mechanical properties as well as the fact that it is bio compatible. The metal lines and contact pads are made out of gold as this material is soft, flexible, has low resistivity and is biocompatible An image of a mesh device can be seen in figure 2.

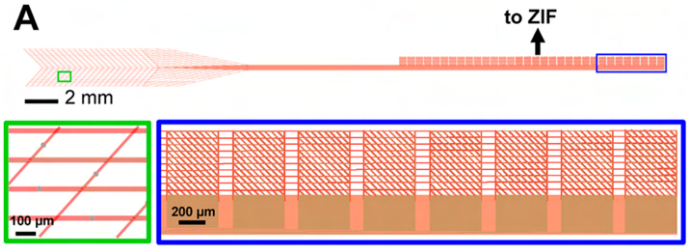

Fig. 2. An overview of a mesh device. In green recording electrodes on mesh part of the device. In blue are the Input output pads where the mesh device can be connected to external electronics [7]

The mesh consists of 3 parts. The input output pads to the ZIF connector, the stem which connects the input-output pads to electrodes and the Mesh Region of the device where the electrodes are located. The electrodes themselves consist of gold and are plated with 10nm chromium and 130nm platinum. The input-output of the design used are designed to be on both on the bottom and top part of the mesh as this makes it easier to interface. [8]

TABLE I
MAPPING OF ELECTRODE RADIUS IN μm TO FIGURE 4

x	35	15	4	4	15	35	x
50	30	10	3	3	10	30	50
45	25	7.5	2	2	7.5	25	45
40	20	5	1	1	5	20	40
Internal Reference	20	5	1	1	5	20	45
45	25	7.5	2	2	7.5	25	45
50	30	10	3	3	10	30	50
x	35	15	4	4	15	35	x

TABLE II
MAPPING OF ELECTRODE TO RECORDING CHANNEL FOR FIGURE 4

x	21	31	41	51	61	71	x
12	22	32	43	53	62	72	82
13	23	33	42	52	63	73	83
14	24	34	44	54	64	74	84
Internal Reference/15	25	35	45	55	65	75	85
16	26	36	47	57	66	76	86
17	27	37	46	56	67	77	87
x	28	38	48	58	68	78	x

B. MEAs

For the design of the MEA's it was decided to make 2 designs with different sizes. Both designs would feature multiple different electrode sizes ranging from $50\mu m$ radius to $1\mu m$ radius. As can be seen in figure 4. Having multiple electrodes sizes on one chip will make it possible for the impedance dependence on radius to be characterized on a single sample. One of these samples would have platinum as the top electrode material. The other design will have gold electrodes.

The mapping of electrode radius of the design in figure 4 can be seen in tables I and II. The other designs feature electrodes of only the same size. The sizes chosen for this were 100 μm, 10μm and 1μm. This was done in order to investigate the effect of electrode size on noise during the neural recordings.

After consultation with the members of the clinical neurophysiology group that carry out the cell cultivation the separation distance between the electrodes was chosen to be 20 μm for designs that feature electrodes of the same size. As this was mentioned to be the approximate size of the neurons.

The metal electrodes arrays were designed to be compatible with the measurement setup which requires that the substrates be of size 48x48mm. The fabrication process was designed to be similar to one used for the mesh device. As such all the metal layer thicknesses are the same.

To provide electrical insulation use was made of SU-8. As it was noticed during the fabrication of the mesh electronics that exposure of SU-8 requires a dose that is 10-20 times higher than that of the standard resists it was decided to minimize the area where of SU-8 was to be patterned. As such only the area that is directly underneath the cultivation chamber was designed to be passivated with SU-8. This shortens the time required for each exposure which improves the throughput of the SU-8 Lithography step.

Initially this passivisation was designed to cover only the top of the layers of the metals underneath the cultivation chamber as well as $1\mu m$ around the metals while leaving the places of the electrodes themselves open.

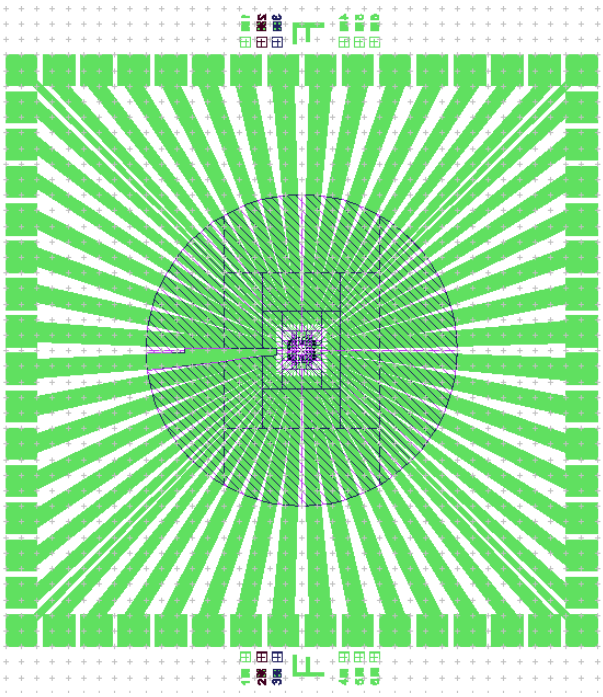

Fig. 3. Overview of mutli radius design file of a MEA device. The electrode array is visible in the center of the design. The purple circle is the SU-8 passivisation where the cultivation chamber will be placed.

IV. FABRICATION

Fabrication was carried out in the MESA+ cleanroom at the university of Twente. For all lithography steps use was made of the Heidelberg MLA150 maskless alligner lithography system. All spin speeds for spincoating were 4000 rpm. The type of SU-8 used throughout this work was 2000-.5. Which when spun at 4000 rpm produces a layer thickness of about 400-500nm thick. Use is made of Lift-off resist (LOR3A) which has a layer thickness of around 300nm when spun at 4000 rpm. And is used in combination with Olin 12 positive resist which creates a layer thickness of 1.2 micron when spun at 4000 rpm.

For all steps that include e-beam evaporation of gold or platinum the typical deposition rate that was aimed for

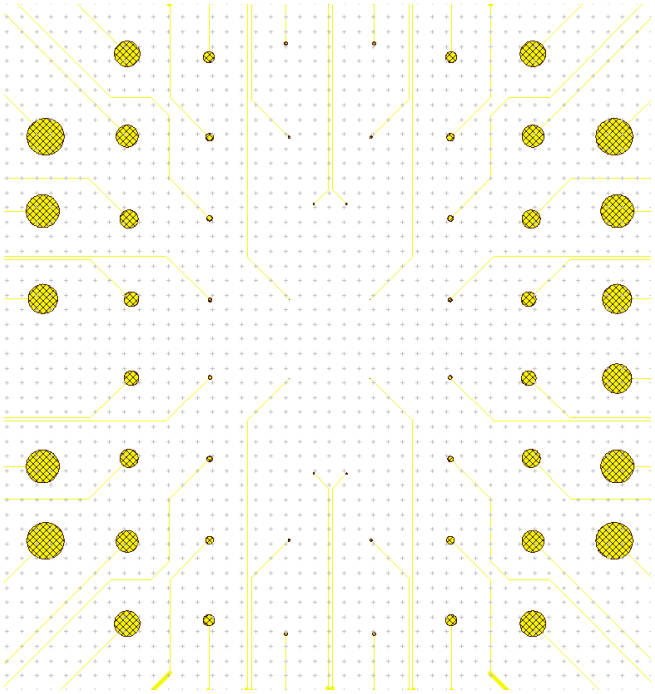

Fig. 4. Design overview of multi electrode array of electrodes with different sizes. The left electrode is left out as the electrode that this would connect to the Reference electrode. The SU-8 layer is not shown for visibility but covers all area except the electrodes themselves

was slightly above .200 nm/s. Typical pressure levels at this rate did not exceed $5 * 10^{-7}$ mbar.

For chromium a typical deposition rate was around .100nm/s. Typical pressure levels were lower than that for gold and platinum as chrome has a gettering effect on the vacuum during processing. Thus helping to trap impurities present in the vacuum thus effectively lowering the process pressure during the evaporation process.

A. Mesh electronics

The fabrication process of the mesh devices can be seen in figure 5.

For all of the e-beam evaporation steps use was made of the BAK600 E-beam evaporator. The BAK600 is capable of processing multiple wafers at once due to it having multiple wafer holders in its processing chamber. All lif-off steps were performed using a solution of RemoverPG. The fabrication procedure for figure 5 is given below.

Step 1-5 define the bottom metal contacts. Step 6 defines the bottom SU-8 layer for the mesh. Step 7-9 define the top metal. Step 10-11 define the top metal electrode. Step 12 creates the top passivisation layer. Step 13 is the release of the device. All masks used for this fabrication can be seen in Appendix A.

1) Silicon Substrate
2) Thermal evapartion of 100nm Ni sacrificial layer

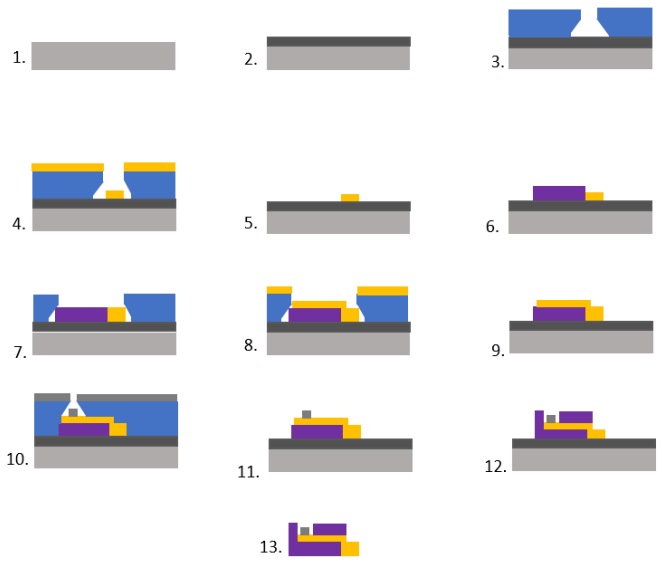

Fig. 5. Fabrication overview for the mesh devices

3) Spincoating of LOR3A, 4000 RPM 45 seconds followed by prebake of 180 degrees for 5 minutes. Followed by spincoating of Olin 12 4000 RPM 30 seconds followed by prebake of 95 degrees for 90 seconds,exposure with MLA 150. Subsequent post bake at 120 degrees for 1 minute development in OPD4262. 30 seconds in the first beaker 90 seconds in the second beaker.
4) Thermal evaporation of 10nm Cr followed by thermal evaporation of 130nm
5) Lift off of Cr/Au layer
6) Spincoating of SU-8 4000 RPM 60 seconds prebake of 65 degrees for 1 minute followed by 95 degrees for 1 minute. Exposure with MLA150 followed by postbake of 65 degrees 1 minute, 95 degrees 1 minute followed by development in RER600 for 2 minutes.
7) Spincoating of LOR3a, Olin 12 and patterning according to step 3
8) Thermal evaporation of 10nm cr followed by thermal evaporation of 130nm au
9) lift-off of Cr/Au layer
10) Thermal evaporation of 10nm Cr followed by thermal evaporation of 130 nm Pt
11) Spincoating of LOR 3a, Olin 12 and patterning according to step 3. e-beam evaporation of 10nm cr followed by 130 nm of platinum. Followed by Lift-off of Cr/Pt layer
12) spincoating and patterning of SU-8 according to recipe in step 6
13) Device release by etching of sacrificial nickel layer using nickel etchant* after oxygen plasma treatment by TePla-300.

* The nickel etchant is made by combining hydrocloric acid, ferriclhoride and DI water in a ratio of 1:1:20 [9].

B. MEA's

For the fabrication scheme for the MEAs can be seen in figure 6. Use was made the of the TOPdamper E-beam evaporation system.

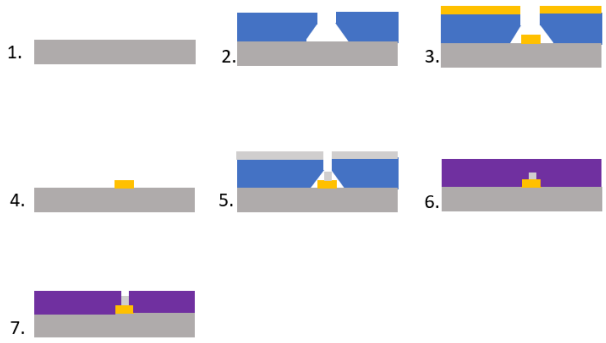

Fig. 6. Schematic of MEA Fabrication

1) Silicon substrate
2) Patterning of LOR3A/Olin 12 according to same recipe
3) E-beam evaporation of 10 nm Cr 130 nm Au
4) Lift off in DMSO.
5) Patterning of LOR3A/Olin 12 followed by e-beam evaporation of 10 nm Cr and 130 nm of pt
6) Patterning of SU-8 2000.5 followed by hard bake

V. Fabrication Issues

This chapter elaborates on several fabrication issues that were encountered during the fabrication of both the mesh electronics and the metal electrode arrays.

A. Mesh electronics

1) Damaged IO lines and electrodes after gold lift off : When production of the Mesh was attempted there was typical failures that occurred consistently throughout such as damaged input output lines. Examples of this can be seen in figure 7.

The cause for this was incomplete exposure of the photoresist this caused by traces of photoresist to still be present. Due to the developer solution dissolving the traces of photoresist underneath the evaporated metal the lines would be damaged as they would lose their adhesion to the bottom layer of SU-8. This problem was solved by making use of the oxygen plasma stripping machine (TePla 300) that descummed the resist removed residual traces of photoresist thus improving the reliabilty of the lift-off.

B. Visible Laser Lines

Throughout the fabrication process laser lines looking like stitches were encountered irregularly throughout the entire fabrication after exposure and development. Initially those were thought to be caused by an insufficient exposure dose

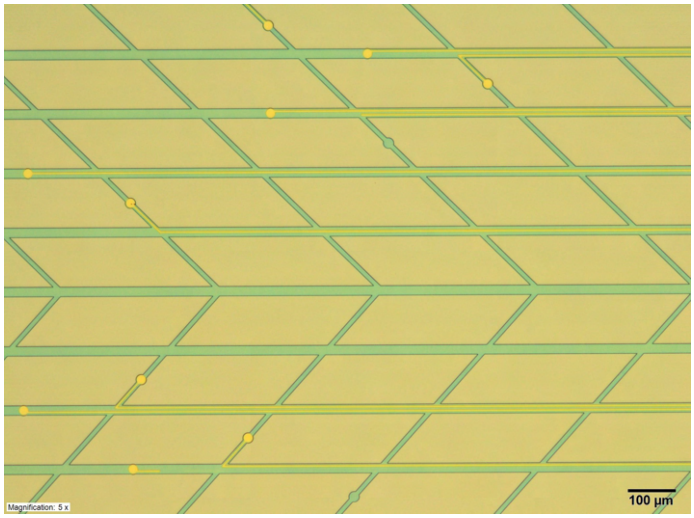

Fig. 7. The mesh part of the device showing interruptions in the gold lines towards the electrodes and missing electrodes.

using the MLA150. Due to the inconsistent occurrence of this effect on samples that went trough the same prepossessing the cause of this issue was attributed to the MLA150.

After the machine was serviced it turned out that the SUI module of the laser writer was defective. This module modulates the width of the laser beam and stretches it to write broader lines wherever the design allows for it. Due to this module being defective the beam can overlap with the previously exposed lines causing extra exposures on the edges of the line profile which makes the resulting developed film look like having stitches as can be observed in figure 8. During the time frame of the only work around for this problem was to increase the exposure dose.

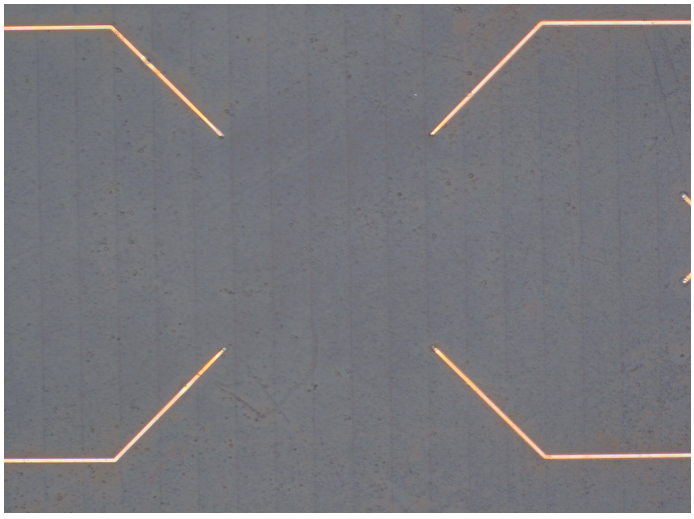

Fig. 8. Example of encountered laser stitches in SU-8 photoresist on glass

C. Poor adhesion of LOR3A during spincoating

When fabrication was commenced a frequently occurring problem was the non uniformity of LOR3A after spin coating as can be seen in figure 9. This would manifest itself mostly in the form of the wafer being uncoated in one or multiple regions at the edges of the wafer and meant that the wafer had to be recoated untill a unifrom coverage was achieved. The solution to this problem was found when use was made of HDMS primer (hexa-dimethylsilane) to improve the the adhesion of SU-8. The use of HMDS was subsequently found to improve the adhesion of LOR3A.

Fig. 9. Wafer spincoated with LOR3A showing non uniform coverage of the wafer.

D. MEAs

1) Substrate: A lot of issues were caused by the substrates chosen for the fabrication. Transparent substrates are preferred for cell cultivation as it allows for the use of phase contrast microscopy such that state and current health of culture can be monitored during cell cultivation. However the transparency of the substrates was found to negatively affect the exposure of the photoresist as the reduced reflectivity resulted in requiring higher exposure doses for successful lithography. The glass substrates also had different surface properties thus affecting resist adhesion.

2) Resist Adhesion: After the switch was made to transparent substrates there was a problem with development of SU-8 photo resist. It was thought that due to the glass substrate being transparent as opposed to silicon substrate which is reflective that the dose was not sufficiently high enough to correctly expose the resist. As such the dose was doubled to 10.000 mJ.

It was then hypothesized that due the substrate being 1mm thick and the fact that glass has less thermal conductivity than silicon [10] [11] That the pre bake times were to not long enough to dry out all the solvent. After increasing the the pre bake and post bake time by 3 minutes photo resist could be observed after development on the gold layers of the substrate. Closer examination showed that SU-8 did in fact adhere partly on the metal surface but not on the glass surface. This can bee seen in figures 10, 11.

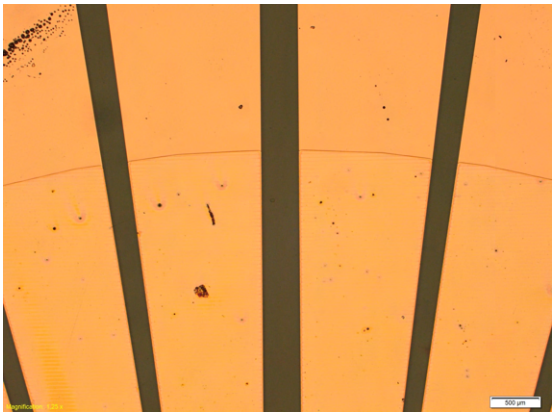

Fig. 10. Microscopy image showing the presence of the SU-8 on the metal electrodes and the absence of it on the glass substrate.

The use of UV-ozone showed slight improvement to

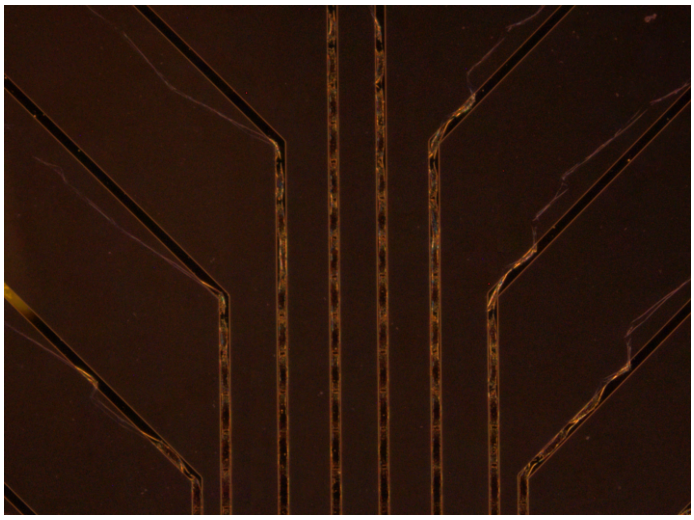

Fig. 11. Dark field microscopy image showing poor adhesion of SU-8 to the gold metal lines

resist adhesion. As such it was thought that adhesion was the main problem. Therefore it was attempted to use HMDS. This resulted in successful development of the SU-8 as can be seen in figure 12 The recipe adjustments that were made to successfully develop SU-8 on glass were:

1) Rinse substrate with Acetone (VLSI), rinse with IPA (VLSI) blow dry with nitrogen.
2) Dehydrate the substrate by baking at 120 degrees for at least 2 minutes. Spin coating of liquid HMDS at 4000 rpm before applying the photoresist
3) Changing the SU-8 pre and post bake times from 1 minute 65 degrees followed by 1 minute at 95 degrees to 1 minute 65 degrees followed by 95 degrees at 3 minutes.
4) Increasing the exposure dose from 5000mJ to 10.000mJ

3) Non uniform quality of platinum layers after lift off: An issue that was frequently noted was that the quality of the platinum electrodes was inconsistent across the the same

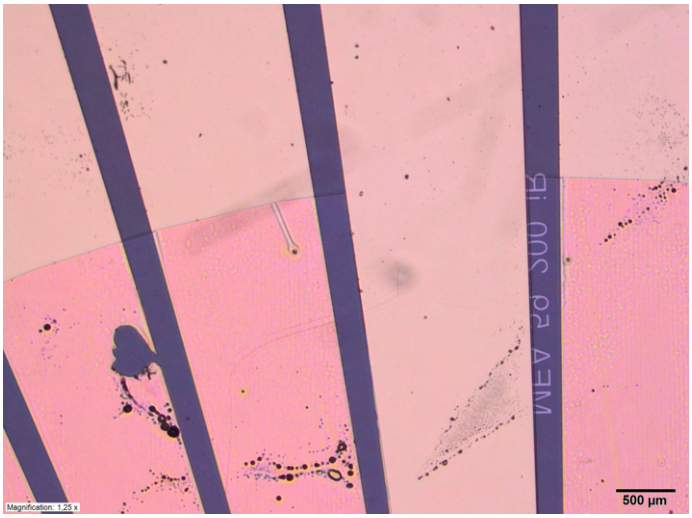

Fig. 12. image showing correct development of SU-8. The SU-8 can be seen on top of the metal and between the metal electrodes. The non coated electrode is the reference electrode which is not designed to have SU-8 on it.

sample. An example of this can be seen in figure 13. It was thought that the black edges that can be seen on most electrodes were due to the platinum not adhering fully to the gold layer underneath. However closer inspection with higher magnification as can be seen in figure 14 seemed to suggest that the platinum does in fact adhere properly and suggest that the black edges are due to a thickness gradient in the platinum layer.

It is unclear at the moment what is the cause of this contamination. It was not possible to verify if this is due to traces of photoresist still being left after the lift-off step as the oxygen plasma machine had broken down.

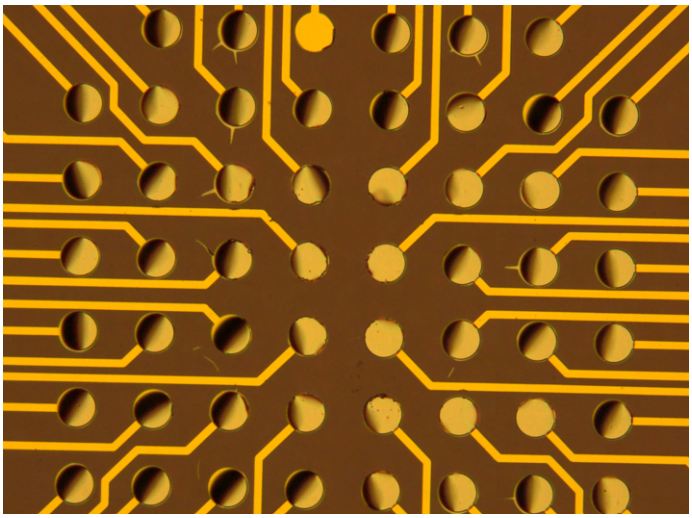

Fig. 13. Inconsistent quality of platinum electrodes across the same sample

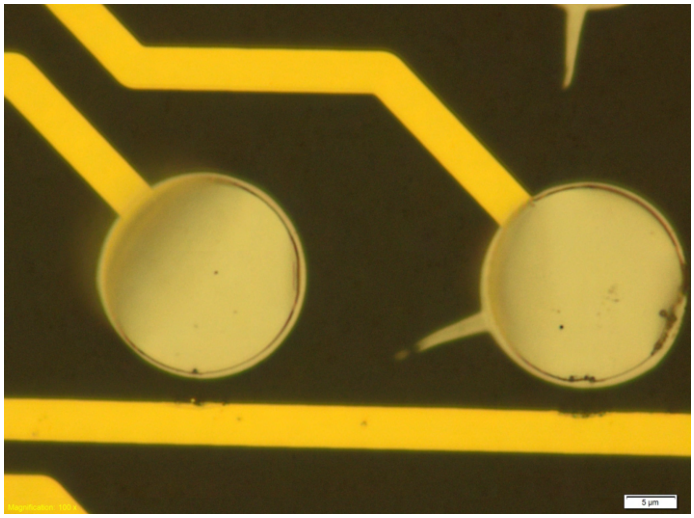

Fig. 14. Microscopy image with higher magnification showing a fading gradient across the platinum electrode

VI. RESULTS

A. Fabrication results

1) Mesh Electronics: Two wafers with 20 mesh devices were fabricated and released. The mesh devices were sealed in bottles and sent to collaborators. To inspect the quality of the mesh devices optical inspection was carried out using microscopy.

Figure 15 shows a separate mesh devices after it had been released by etching of the sacrificial nickel layer. The devices were sucked out the solution one be one with the use of a syringe and transferred multiple times trough DI water to dissolve the etchant. The devices were then transferred to glass slides to be imaged by microscope.

2) MEAs: Two devices were successfully made. The successfully fabricated designs were an all $1\mu m$ Platina electrode array and a multi radius design of only gold electrodes. Their impedances were measured and cells were cultivated on top of them.

B. Impedance Measurements

For the impedance measurements use was made of the setup of the clinical neuropshysiology group at the University of Twente. To use the setup a plastic ring is placed on top of the MEA and filled with PBS. For the reference electrode an Ag/AgCl wire is used as an external reference electrode which is placed in the PBS solution. The setup measures the attenuation and phase shift of the electrodes to determine their impedance.

A more elaborate description of this setup and it operation can be seen in appendix B.

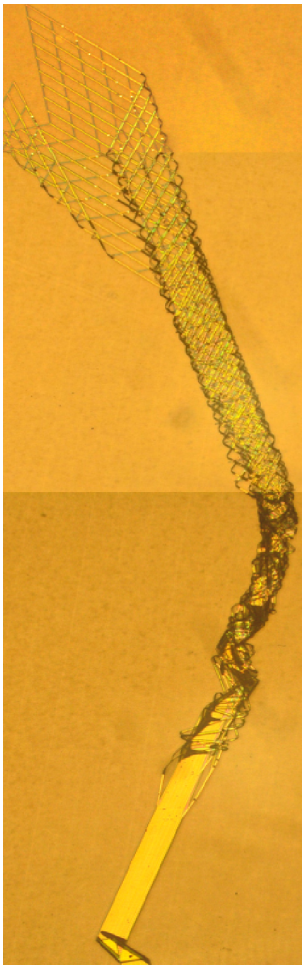

Fig. 15. A released mesh device having coiled up around itself.

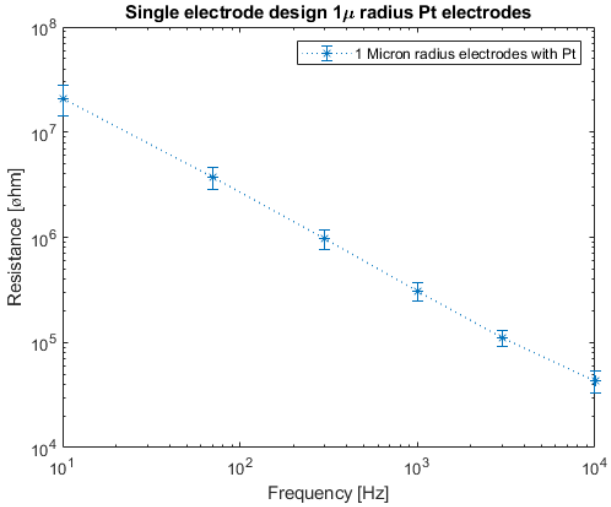

Fig. 16. Measured mean impedance vs frequency for MEA of $1\mu m$ Pt electrodes with standard deviation

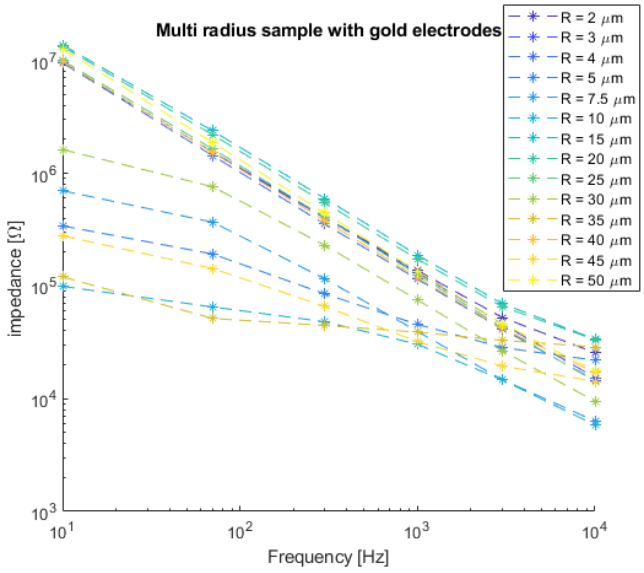

Fig. 17. Measured impedance vs frequency for multi radius sample. The results are averaged for each radius.

Figure 16 shows the mean impedance vs frequency for a sample that contained 59 electrodes with $1\mu m$ radius of platinum on top of the gold electrodes with standard deviation. The measured impedances for the multi electrode design can be seen in figure 17. As there were multiple electrodes with the same radius the measured impedance vs frequency behaviour for electrodes of the same radius was averaged.

C. Cell cultivation

Cells were cultivated on the substrates by the clinical neurophysiology group of the University of Twente. To do this a group of isolated cells from a baby rat is placed in a cultivation chamber which is glued on top of the MEA after it has been sterilized.

The activity of the cells and RMS noise was then measured using a MEA2100-system from multichannel systems for 10 minutes. The setup uses a Bessel filter with a bandwidth of 3kHz. The results for those measurements can be seen in figures, 18 and 19.

VII. Discussion

From figure 17 we can see that there is dependence of impedance. When looking closely it can be seen that the smallest electrodes measured a lower value impedance value than some of the electrodes with a bigger radius. This is not in according to expectation as one expects the impedance to scale inversely proportional with surface area. Thus one would expect the impedance to scale quadratically with decreasing radius which is clearly not observed. With only 4 electrodes per size the data is not quantitative enough to make any hard claims about the measured size dependence nor on the reliability of the measurement setup.

The obtained impedance from figure 16 for the 1 μm seems higher than that of 17. However due to a the mistake in the design file for the gold sample the smallest 4 electrode

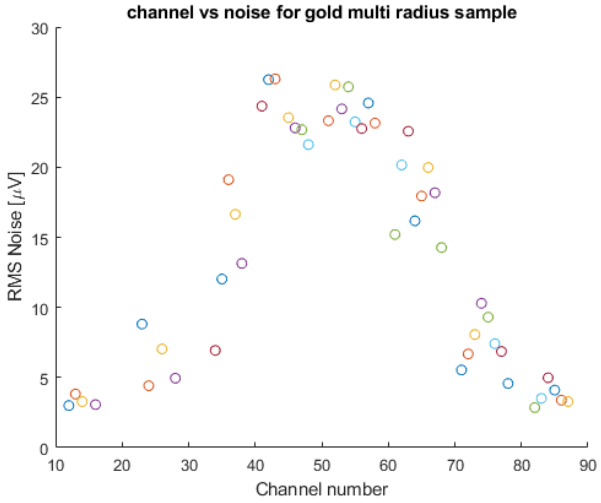

Fig. 18. Channel number vs measured noise for multi radius gold sample

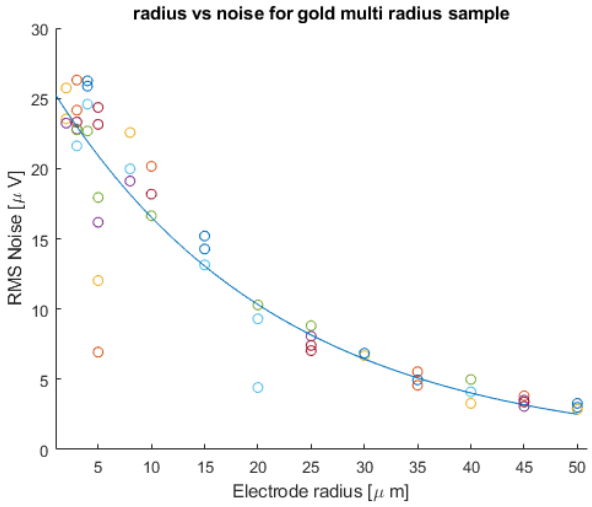

Fig. 19. Electrode radius vs measured RMS noise with exponential fit

sizes where $1\mu m$ bigger than was planned. There is also the fact that the platinum sample might have been damaged due to the oxygen plasma. This means it is not possible to make a one to one comparison for the $1\mu m$ platinum sample with gold.

Figures 18 and 19 look promising as figure 18 shows symmetry which is consistent with the symmetry of the device. Figure 18 shows an exponential dependence of RMS noise on electrode radius which is not in agreement with the expected scaling of noise on electrode radius.

VIII. Conclusion

In this paper the fabrication of mesh electronics and MEA's is presented. As well as impedance characterization results of 2 successfully fabricated MEA's containing 59 $1\mu m$ electrodes coated with platinum and a multi radius electrode design with gold electrodes. In addition cells were successfully cultivated on these designs to study their performance in vitro. The Mesh devices were successfully fabricated and the devices were sent to collaborators in Nijmegen.

Two MEA's have succesfully been fabricated. Impedance measurements were performed on both devices however the current data set is not quantitative enough to make any substantiated claims about the impedance dependence on size nor to make any claims on the effect of platinum on the performance of the electrodes. The current impedance measurements show spread and a consistent relation between impedance and radius has not been identified. As such more work is needed to identify the cause of this spread.

The measured noise dependence on electrode radius shows exponential behaviour. This is not in line with expectation nor is it in accordance with literature results [12]. It is not known what the cause of this discrepancy is. Additional work should be done to verify if the measurement is repeatable and that it is free of external noise sources.

Furthermore the presented solution for the SU-8 and LOR3A photoresist adhesion problems with the use of HMDS has helped to improve reliability of the fabrication process.

IX. Recommendations

A lot of time was spent inefficiently by relying on the MLA150 for the exposure of SU-8. It is therefore recommended that the non critical processing of the SU-8 exposure is to be done with the EVG6200NT lithography system of the cleanroom. This is expected to provide more consistency than the maskless aligner and should decrease the production time.

Regarding the impedance measurement setup there is not enough data to give concrete recommendations on how it could be improved. The fact that the sample sustained damage from the oxygen plasma makes it impossible to attribute this spread to the measurement setup or non uniformity of the sample. As such it is recommended to redo this measurement with a new undamaged sample.

It is suggested to investigate the use of the HMDS oven to apply HMDS to the substrates in a vapour form instead of spincoating it on the samples. The subsequent baking steps when HMDS is spun in the liquid phase causes the excess HMDS to form ammonia which can diffuse trough resists and develop them before exposure. It requires further research to see if this is beneficial for the quality of the platinum layers. [13]

References

[1] G. Hong and C. M. Lieber, "Novel electrode technologies for neural recordings," *Nature Reviews Neuroscience*, vol. 20, no. 6, pp. 330–345, Mar. 2019. [Online]. Available: https://doi.org/10.1038/s41583-019-0140-6

[2] V. S. Polikov, P. A. Tresco, and W. M. Reichert, "Response of brain tissue to chronically implanted neural electrodes," *Journal of Neuroscience Methods*, vol. 148, no. 1, pp. 1–18, Oct. 2005. [Online]. Available: https://doi.org/10.1016/j.jneumeth.2005.08.015

[3] T.-M. Fu, G. Hong, T. Zhou, T. G. Schuhmann, R. D. Viveros, and C. M. Lieber, "Stable long-term chronic brain mapping at the single-neuron level," *Nature Methods*, vol. 13, no. 10, pp. 875–882, Aug. 2016. [Online]. Available: https://doi.org/10.1038/nmeth.3969

[4] T. Chung, J. Wang, J.-Y. Wang, B. Cao, Y. Li, and S. Pang, "Electrode modifications to lower electrode impedance and improve neural signal recording sensitivity," *Journal of neural engineering*, vol. 12, p. 056018, 09 2015.

[5] N. Wu, S. Wan, S. Su, H. Huang, G. Dou, and L. Sun, "Electrode materials for brain–machine interface: A review," *InfoMat*, vol. 3, no. 11, pp. 1174–1194, 2021. [Online]. Available: https://onlinelibrary.wiley.com/doi/abs/10.1002/inf2.12234

[6] D. R. White, R. Galleano, A. Actis, H. Brixy, M. D. Groot, J. Dubbeldam, A. L. Reesink, F. Edler, H. Sakurai, R. L. Shepard, and J. C. Gallop, "The status of johnson noise thermometry," *Metrologia*, vol. 33, no. 4, pp. 325–335, Aug. 1996. [Online]. Available: https://doi.org/10.1088/0026-1394/33/4/6

[7] G. Hong, R. D. Viveros, T. J. Zwang, X. Yang, and C. M. Lieber, "Tissue-like neural probes for understanding and modulating the brain," *Biochemistry*, vol. 57, no. 27, pp. 3995–4004, Mar. 2018. [Online]. Available: https://doi.org/10.1021/acs.biochem.8b00122

[8] J. M. Lee, G. Hong, D. Lin, T. G. Schuhmann, A. T. Sullivan, R. D. Viveros, H.-G. Park, and C. M. Lieber, "Nanoenabled direct contact interfacing of syringe-injectable mesh electronics," *Nano Letters*, vol. 19, no. 8, pp. 5818–5826, Jul. 2019. [Online]. Available: https://doi.org/10.1021/acs.nanolett.9b03019

[9] T. G. S. Jr., T. Zhou, G. Hong, J. M. Lee, T.-M. Fu, H.-G. Park, and C. M. Lieber, "Syringe-injectable mesh electronics for stable chronic rodent electrophysiology," *Journal of Visualized Experiments*, no. 137, Jul. 2018. [Online]. Available: https://doi.org/10.3791/58003

[10] A. C. Sparavigna, "Thermal Conductivity of the Crystalline Silicon," *Philica*, p. 1143, 2017. [Online]. Available: https://hal.science/hal-01626126

[11] "Thermal conductivity table." [Online]. Available: http://hyperphysics.phy-astr.gsu.edu/hbase/Tables/thrcn.html

[12] J. Scholvin, J. P. Kinney, J. G. Bernstein, C. Moore-Kochlacs, N. Kopell, C. G. Fonstad, and E. S. Boyden, "Close-packed silicon microelectrodes for scalable spatially oversampled neural recording," *IEEE Transactions on Biomedical Engineering*, vol. 63, no. 1, pp. 120–130, Jan. 2016. [Online]. Available: https://doi.org/10.1109/tbme.2015.2406113

[13] M. Corporation, "Adhesion promotion hmds," -, july, 2023. [Online]. Available: https://www.microchemicals.com/products/adhesion_promotion/hmds.html

[14] *Low cost low power instrumentation amplifier AD620*, Analog Devices, 7 2022, rev. D.

APPENDIX A
MASK DESIGNS

Mesh devices

Figures 20 ,21 ,22, 23 show the design files used for the fabrication of the mesh devices.

Fig. 20. Mask 1 the bottom metal contact pads

Fig. 21. Mask 2 the bottom SU-8 layer corresponding to 6 in figure 5

Fig. 22. Mask 3 corresponding to step 7 in figure to pattern the metal lines 5

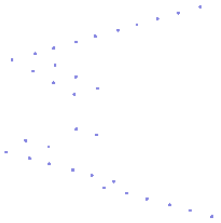

Fig. 23. Mask 4 to pattern the platinum electrodes corresponding to 10 in figure5

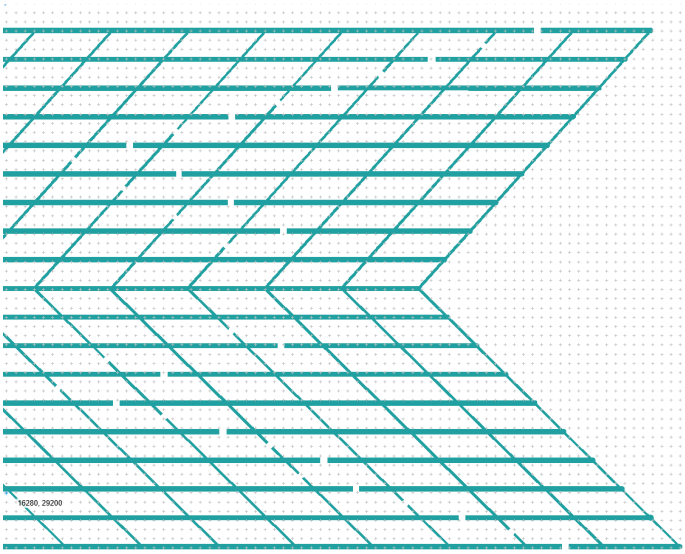

Fig. 24. Mask 5 to apply the top passivation while leaving the top electrodes open corresponding to 12 in figure5

A. MEA designs

All MEA designs that were not shown in the main body can be seen in figures 25 ,26 and 27

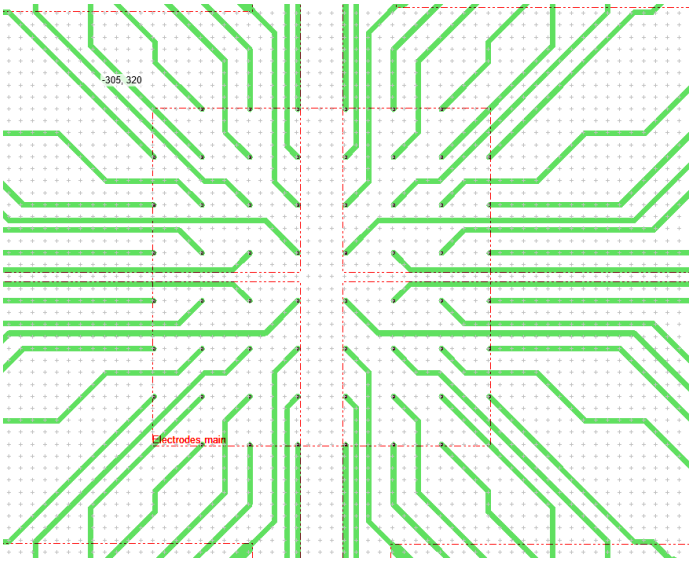

Fig. 25. 1 micron radius design

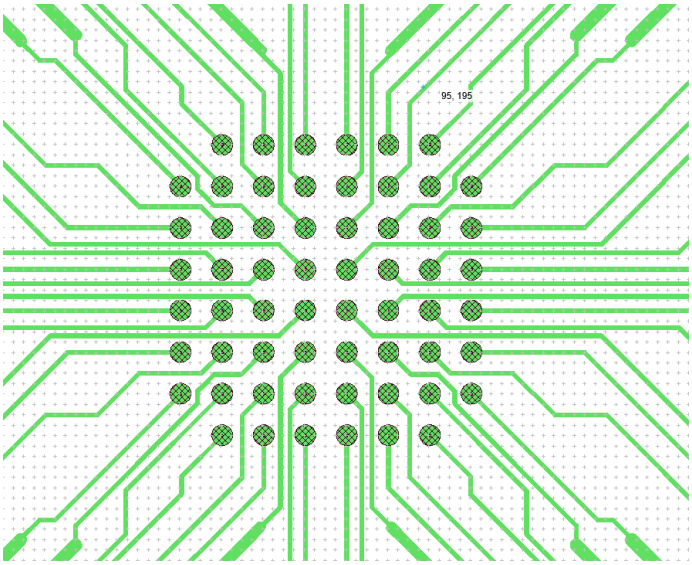

Fig. 26. 10 micron radius design

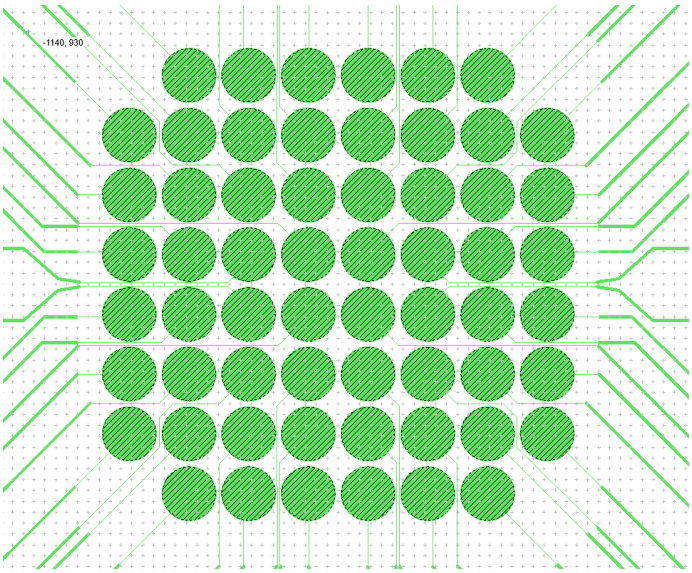

Fig. 27. 100 micron electrode design

APPENDIX B

IMPEDANCE MEASUREMENT SETUP

For impedance measurements use is made of the setup 1 of the clinical neuropsyschology group of the university of Twente. It consist of the following hardware:

1) MEA 1060-INV-BNC (figure 28)
2) MEA amplifier from multichannel systems
3) MEA stimulus Generator (STG 1002 from Multi Channel Systems)
4) HP3245A signal generator
5) PL303QMD Quad-Mode Duel Power Supply
6) Amplifier board featuring an AD620 instrumentation amplifier as can be seen in figure 29.

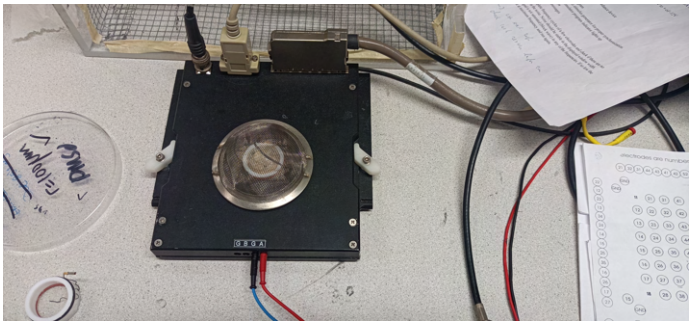

Fig. 28. Mea base plate in which the measurement sample is placed.

The impedance measurements are performed using a Labview program.

The setup to operates in the following manner. The HP3245 signal generator generates a sine wave at the frequency of measurement this is then passed into the left port of the amplifier board. Which is also connected to the MEA amplifer and to the MEA 1060-INV-BC which holds the measurement sample. The signal that is fed into the MEA is then returned to the amplifier which amplifies it and then outputs this to the same MEA Amplifier. The phase shift and amplitude are then found by fitting to the same sine wave. Which performs corrections for a delay by sampling frequency, the input impedance of the opamp and a shunt capacitance. Then it continues sweeping the frequency and then moves on to the next electrode until it finishes measuring all electrodes.

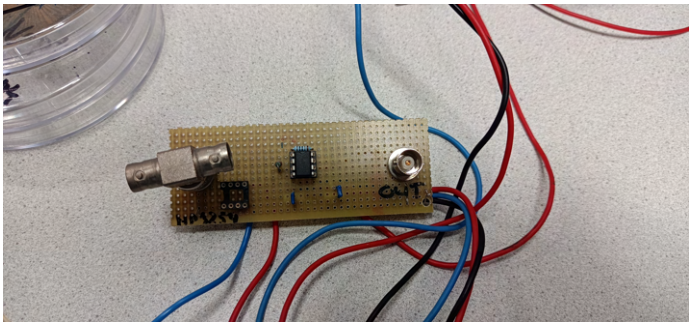

Fig. 29. Amplifier board featuring an AD620 instrumentation amplifier from the layout of the board it seems that the input signal is fed directly in to the MEA 1060-INV-BNC and then the attenuated signal is amplified. From its datsheet and the value of the gain resistor of 1kΩ the gain value of the amplifier is 50.40

APPENDIX C
CODE

All data analysis and processing was done with MATLAB Code used for processing the impedance measurement for gold multi electrode sample.

```
close all
clear all

data = readmatrix("855.csv")
test = data(4:4:240,2:end)
skips = [0 1 2 3]

badchannel = sort([22,33,21,32,31,27,17,25])
badindex = repelem(badchannel,4)
skipsadd = repmat(skips,1,length(badchannel))
badindices = badindex + skipsadd +5
goodindex = setdiff(1:length(data), badindices)

%avg = mean(data(([2:4:238 4:4:240]),2:end),[2 6])
c= parula(100)
% loglog(data(1,2:end),)
% j = 0
% bad = [0]
% for i = 1:1:length(test)
%     if any(test(i,1)-badchannel==0)
%         bad(j+1) = i
%
%
%     end
% end
alldata= data(4:4:240,1:end)
gooddata=data(goodindex,:)
%badi =zeros(1,length(badchannel))
ter = alldata(:,1)
badi = zeros(1,length(badchannel))
for i = 1:1:length(badchannel)
    badi(i)= find(badchannel(i)==ter)

end
% [row,column] = ismember(test, badchannel)
size = [50,45,40,40,45,50,35,30,25,20,20,25,30,35,15,10,7.5,5,5,7.5,10,15,5,4,3,2,2,3,4,5]
sizes = [size flip(size)]
un =  unique(size)
%plot(data(1,2:end),test)
line_color = ['b','g','c','m','y','k']
for i =1:1:length(un)
    k = un(i);
    m = find(sizes==k)
    l = setdiff(m,badi)
    temp=mean(test(l,1:end))
    hold on
    txt = ['R = ',num2str(k),' \mum']
    e = plot(data(1,2:end),mean(data(1,2:end)),'color',c(7*i,:),'DisplayName',txt)
    e.Marker = '*';
    e.LineStyle = "--"
    title("Multi radius sample with gold electrodes")
    xlabel('Frequency [Hz]')
    ylabel('impedance [\Omega]')
```

```
    set(gca,'Yscale','log')
    set(gca,'Xscale','log')
end
legend show
hold off
figure(3)
for i =1:1:length(un)
    k = un(i);
    ka = zeros(1,6)+k
    l = find(sizes==k)
    temp=mean(test(l,1:end))
    hold on
    txt = ['R = ',num2str(k),' \mum']
    f = plot(ka,data(1,2:end),mean(test(l,1:end)))
    f.Marker = '*';
    f.LineStyle = "--"
   % xlabel('Frequency [Hz]')
    %ylabel('impedance [\Omega]')
    set(gca,'Xscale','log')
    set(gca,'Yscale','log')
end
view(3)
legend show
```

Code used for processing noise data from 2100MEA setup for both samples. The data is manually imported into MATLAB.

```
    close all
badchannel = sort([22,15,33,21,32,31,27,17,25,44])

for i = 12:87
    if ismember(i, badchannel)
    else
    find(Cs==i)
    hold on
    scatter(i,mean(Ns(Cs==i)))
    xlabel("Channel number")
    ylabel("RMS Noise [\muV]")
    title("channel vs noise for gold multi radius sample")
    disp(std(Ns(Cs==i)));
    end

end
hold off
B=[50,45,40,35,30,25,20,15,10,8,5,4,3,2,1];
A=[12,13,14,21,22,23,24,31,32,33,34,41,42,43,44];

C=[50,45,40,40,45,50,35,30,25,20,20,25,30,35,15,10,8,5,5,8,10,15,5,4,3,2,2,3,4,3];
D = flip(C);
E =[C,D];
j=0;
Data = zeros(1,60)
Radius = zeros (1,60)
figure(2)
skipped = 0
for i = 12:87
    if ismember(i, badchannel)
        skipped = skipped+1;
    else
    k = find(Cs==i);
    if isnan(mean(Ns(k)==NaN))

    else
        j=j+1;
        hold on
        scatter(E(1,j+skipped),mean(Ns(k)));
        Data(1,j)=mean(Ns(k));
        Radius(1,j)=E(1,j+skipped);
        drawnow

    end
    xlabel("Electrode radius [\mu m]")
    ylabel("RMS Noise [\mu V]")
    title("radius vs noise for gold multi radius sample")
    xlim([1,51])
    end
end
figure(3)
scatter(E,Data)
Kt= 4.11*10^(-21)

R = (Data*10^(-6).^2)/(4*Kt*3000)
figure()
```

```
scatter(E,R)
```

code used for processing impedance measurements on $1\mu m$ radius platina sample

```
    close all
clear all

data = readmatrix("no12_10 micron.csv")
%
% loglog(data(1,2:end),data(2:2:end,2:end))
% figure()
% loglog(data(1,2:end),)


avg = mean(data(2:2:240,2:end))
Sd = ones(size(6))*std(data(2:2:240,2:end))
    loglog(data(1,2:end),data(2:2:240,2:end))
grid on
figure()
plot(data(1,2:end),avg)
figure
e =errorbar(data(1,2:end),avg,Sd,'Linestyle', ':')
xlabel('Frequency [Hz]')
ylabel('Resistance [\ohm]')
set(gca,'Yscale','log')
set(gca,'Xscale','log')
legend('1 Micron radius electrodes with Pt')
title(' electrode design 1\mu radius Pt electrodes')
e.Marker = '*';
```